International Journal of Nanomedicine

Dovepress
open access to scientific and medical research

Open Access Full Text Article

ORIGINAL RESEARCH

A Cosmeceutical Topical Water-in-Oil Nanoemulsion of Natural Bioactives: Design of Experiment, in vitro Characterization, and in vivo Skin Performance Against UVB Irradiation-Induced Skin Damages

Carol Yousry[1], Mona M Saber[2], Wessam H Abd-Elsalam[1]

[1]Department of Pharmaceutics and Industrial Pharmacy, Faculty of Pharmacy, Cairo University, Cairo, Egypt; [2]Department of Pharmacology and Toxicology, Faculty of Pharmacy, Cairo University, Cairo, Egypt

Correspondence: Wessam H Abd-Elsalam, Department of Pharmaceutics and Industrial Pharmacy, Faculty of Pharmacy, Cairo University, Cairo, Egypt, Email wessam.hamdy@pharma.cu.edu.eg

Introduction: Damage to human skin occurs either chronologically or through repetitive exposure to ultraviolet (UV) radiation, where collagen photodegradation leads to the formation of wrinkles and skin imperfections. Consequently, cosmeceutical products containing natural bioactives to restore or regenerate collagen have gained a remarkable attention as an ameliorative remedy.

Methods: This study aimed to develop and optimize collagen-loaded water-in-oil nanoemulsion (W/O NE) through a D-optimal mixture design to achieve an ideal multifunctional nanosystem containing active constituents. Vit E was included as a constituent of the formulation for its antioxidant properties to minimize the destructive impact of UV radiation. The formulated systems were characterized in terms of their globule size, optical clarity, and viscosity. An optimized system was selected and evaluated for its physical stability, in vitro wound healing properties, and in vivo permeation and protection against UV radiation. In addition, the effect of collagen-loaded NE was compared to Vit C-loaded NE and collagen-/Vit C-loaded NEs mixture as Vit C is known to enhance collagen production within the skin.

Results: The optimized NE was formulated with 25% oils (Vit E: safflower oil, 1:3), 54.635% surfactant/cosurfactant (Span 80: Kolliphor EL: Arlasolve, 1:1:1), and 20.365% water. The optimized NE loaded with either collagen or Vit C exhibited a skin-friendly appearance with boosted permeability, and improved cell viability and wound healing properties on fibroblast cell lines. Moreover, the in vivo study and histopathological investigations confirmed the efficacy of the developed system to protect the skin against UV damage. The results revealed that the effect of collagen-/Vit C-loaded NEs mixture was more pronounced, as both drugs reduced the skin damage to an extent that it was free from any detectable alterations.

Conclusion: NE formulated using Vit E and containing collagen and/or Vit C could be a promising ameliorative remedy for skin protection against UVB irradiation.

Keywords: water-in-oil nanoemulsion, collagen, vitamin C, vitamin E, fibroblast, UVB irradiation

Introduction

Collagen is a major structural protein that forms most of the connective tissue, and thus functions as a support network to the cellular structures. collagen is available in the dermis layer of the skin, where the dermal fibroblasts produce the distinct polypeptide chains of types I and III collagen as precursor molecules (Procollagen).[1] It was found that the dermis comprises mainly type I collagen (85–90%) and lesser quantities of type III collagen (10–15%).[2] In general, both the abundance and strength of collagen are directly related to the healthy appearance of the skin, including hydration, smoothness, and luminosity.[3]

Received: 23 February 2022
Accepted: 27 June 2022
Published: 6 July 2022

Damage to human skin occurs either over time (chronologic aging) or through repetitive exposure to solar ultraviolet (UV) radiation (photoaging). Chronologic aging or skin aging is a normal consequence of the damage of the collagen fibers over time, where the skin loses its thickness and strength.[4] On the other hand, photoaging occurs as a result of exposure to solar UV radiation, which is composed of UVA (320–400 nm), UVB (280–320 nm), and UVC (200–280 nm).[5] UVB was found to be responsible for the majority of the injury to the skin, as it is absorbed by the epidermis and brings about damage to the DNA by producing harmful photoproducts. Besides, UVB reacts with the water content of the skin generating reactive oxygen species (ROS) which interact with cellular lipids and proteins, resulting in apoptosis and genetic mutations.[6] Moreover, ROS were found to trigger proteases in human skin that upregulate the production of matrix metalloproteinases (MMPs), which by their role destroy collagen.[7] Photoaged skin is characterized by coarse wrinkles, dyspigmentation, and telangiectasia.[2] As illustrated in Figure 1, the healthy skin of a rat (Figure 1A) showed some defects upon exposure to UVB radiation (Figure 1B), where skin alterations such as erythema and wrinkles, as well as, hyperpigmentation in certain areas were observed.

In context with these facts, vitamin C (Vit C), in its most biologically active form; L-ascorbic acid, has shown to possess anti-aging effects by enhancing collagen production and stabilizing its fibers, thus lessening collagen degradation.[8] In addition, Vit C has antioxidant properties via reducing the formation of ROS such as hydroxyl radicals, superoxide radicals, and singlet oxygen.[6] Also, Vit C was proved to minimize melanin formation, therefore dropping skin pigmentation.[9] However, Vit C is photochemically unstable, where it gets oxidized to dehydro ascorbic acid, which imparts a yellow color upon exposure to light.[10] To circumvent the stability issues of vitamin C, previous formulation approaches were to lower the pH of the medium or limit the water content.[11]

In a parallel line, the use of vitamin E (Vit E) in the protection against oxidative damage caused by UV radiation is well established as per its antioxidant properties, and it has been incorporated in many antioxidant cocktails, along with other ingredients to minimize the destructive impact of UV radiation by heightening the antioxidative capacity of the epidermis.[12] Furthermore, fibroblast attachment, proliferation, and collagen secretion were enhanced in the presence of Vit E.[13]

Nanoemulsions (NEs) are colloidal systems usually employed in the nutraceutical, pharmaceutical, and cosmetic industries.[14] NEs are isotropic thermodynamically stable nanoformulations that are characterized by a fast onset of action with improved drug efficacy, effortless preparation and scale-up, and act as a cargo shield against hydrolysis and oxidation.[15–17] In addition, NEs are well-tolerable by the skin, with a skin-friendly appearance, in addition to their suitability for accommodating hydrophilic and lipophilic drug substances.[18] Consequently, NEs have become famous for dermal drug delivery, adding to the existence of surfactants in their composition, which in turn surges the membrane

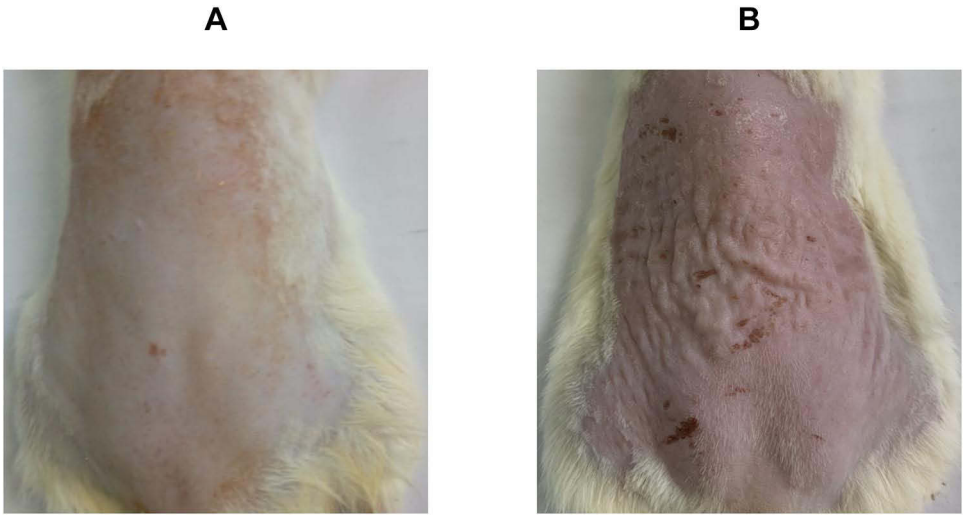

Figure 1 Rats' dorsal skin photographs of (**A**) normal control group (unexposed to UVB-irradiation) and (**B**) positive control group (exposed to UVB-irradiation, where skin alterations were visible, as the skin was erythematous and wrinkled, as well as, being hyperpigmented in certain areas).

permeability and circumvents the skin barrier, thus facilitating drug transport through the skin.[19] NEs are usually prepared using a random formulation approach, which is based on trial and error and lacks a cause–effect relationship between independent variables and dependent response, leading to an erratic and a non-optimized formulation. On the contrary, the formulation of NEs on basis of a validated statistical experimental design results in reliable outcomes and realistic evaluations of the impact of different variables on the formulation process. Numerous studies including different statistical experimental designs for formulating NEs have been established and among them, the D-optimal mixture design. This type of design allows the formulator to apply a limitation that the sum of all components is constant (ie, 100% w/w), which is a typical feature related to the pseudo-ternary phase diagram plotted to contour NEs regions.[20]

Based on all the above-stated pieces of evidence, collagen has been introduced as a counteracting therapy in different cosmetic formulations owing to its high biodegradability, biocompatibility, and non-toxicity,[21] and to boost the valuable effect of collagen on the skin, rethinking a multifunctional nanosystem that co-deliver collagen along with multi-antioxidant vitamins such as Vit C and E would be beneficial. Taking into consideration the aforementioned properties of NEs, employing them as a water-in-oil (W/O) NE for hydrophilic actives such as collagen or Vit C seems reasonable to improve their stability and enhance their permeation and thus boosting their efficacy. Thus, the primary objective of this study was to develop and optimize the formulation of collagen-loaded W/O NE through a D-optimal mixture design and select an optimized formulation. The oily phase was suggested to be a mixture of the natural oils; safflower oil and Vit E, while Span 80 and Kolliphor EL were incorporated as a surfactant, and Arlasolve was used for the first time as a cosurfactant in the formulation of NE. Safflower oil is an edible oil that is obtained from safflower seeds, and it comprises various bioactive compounds such as linoleic acid, tocopherols, sterols, squalene hydrocarbons, and polyphenols.[22] The safflower seed oil has been recommended to be used as a promoter of skin barrier homeostasis, in addition, safflower has shown different physiological functions, including antioxidation and melanin production inhibition.[23] The inclusion of dermally safe surfactants is crucial in formulating topical skin formulations, where surface-active agents with structure blocks of natural origin are frequently considered to be more biocompatible and biodegradable compared to chemically created counterparts. An add-on property that minimizes the skin sensitization potential and favors their usage for dermal application is being uncharged or nonionic.[24] Span 80 is a non-ionic lipophilic surfactant with an HLB value of 4.3, which is composed of a natural fatty acid (oleic acid) and sugar alcohol sorbitol,[24] while Kolliphor EL, polyoxyl 35 castor oil, is a nonionic surface-active agent (HLB value = 12–14).[25] Arlasolve is 3,6-dimethoxy-2,3,3a,5,6,6a-hexahydrofuro[3,2-b]furan, that acts as a skin adjuvant by boosting the performance and enhancing the delivery of actives within formulations for many personal care applications. To test the boosted permeation character of the developed system, the permeation of the optimized NE was investigated through a confocal laser scanning microscopy study. The secondary objective was to load the optimized NE with Vit C and to compare its effect with that of collagen or a mixture of both collagen- and Vit C-loaded NEs on fibroblast cell lines, namely normal human fibroblast (HFB4) and Baby Hamster Kidney fibroblasts (BHK). In addition, an in vivo study and histopathological investigations were conducted to verify the hypothesis of the skin protection outcome of the optimized formulations against UVB irradiation in Wistar rats.

Materials and Methods

Materials

Porcine type-I collagen (Cell matrix Type I-A), safflower seed oil (*Carthamus tinctorius*), Vitamin E (α-tocopherol), Span 80 (Sorbitan monooleate), Kolliphor EL, vitamin C (L-ascorbic acid), and Rhodamine B dye were acquired from Sigma Aldrich (Missouri, USA). Arlasolve was obtained from Croda International Plc (East Yorkshire, UK). Any other used chemicals were of high purity and used as received.

Construction of Pseudo-Ternary Phase Diagrams

According to the outcomes of the preliminary trials (data not shown), vitamin E and safflower oil (1:3) represented the oily phase, Span 80, and Kolliphor EL (1:1) were selected as surfactants, while Arlasolve was used as a cosurfactant. The selected surfactants were mixed with the cosurfactant at a ratio of 2:1 to form S/Cos mixture, which was further blended

with the oily phase at weight ratios of 90:10, 80:20, 70:30, 60:40, 50:50, 40:60, 30:70, 20:80, and 10:90. Nanoemulsions (NEs) were prepared using the aqueous titration method, where water was added dropwise to the formed blends under vortexing (Stuart variable speed vortex mixer/SA8; UK) till the last point the system was transparent and clear. The concentrations of the different ingredients (as percentages) were plotted on a pseudo-ternary phase diagram, and the borders of the clear zone were determined.

Design of Experimentation (DOE)

Design Expert® software (version 7.0.0, Stat-Ease Inc., Minneapolis, USA) was employed to create a D-optimal mixture design aiming to provide maximized prediction power in the designated cluster of 16 experimental runs, thus lessening any possible variance correlated to the estimations of the coefficients in the model. The independent variables were set so that the percentage of the oils (A) ranges from 20% to 45%, the percentage of the surfactant/cosurfactant (S/Cos) (B) lies between 45% and 70%, and the percentage of water (C) fall within range 10–25%.

The prepared runs were characterized according to the dependent variables, which were selected to include the globule size (GS) (Y_1) in nm, polydispersity index (PDI) (Y_2), the percent transmittance (%T) (Y_3), and viscosity (Y_4) in cp. The resultant linear, quadratic, cubic, and special cubic mathematical models were analyzed by the software. The value of standard deviation (SD), R^2, adjusted R^2, predicted R^2, and the predicted residual error sum of squares (PRESS), as statistical parameters, were compared to test the significance of the model, where the one with the higher values of R^2, adjusted R^2, and predicted R^2, and with a difference of less than 0.2 (between the adjusted R^2 and the predicted R^2) was chosen. On the contrary, the least SD and PRESS values were targeted. The composition and the responses of the suggested experimental runs, loaded with collagen (1% w/w), are represented in Table 1. The optimized NE was elected by the software, in which the GS (Y_1) and PDI (Y_2) were minimized, while %T (Y_3) and viscosity (Y_4) were maximized. The optimized NE was prepared and loaded with either collagen or Vit C (both at a concentration of 1% w/w) to compare the effectiveness of the carrier to deliver both actives, as Vit C is known to be a viable supplement to enhance collagen synthesis and accelerate soft tissue healing.

Table 1 The Composition of the Experimental Runs According to the D-Optimal Statistical Design and Their Responses

Runs	A Oils (%)	B S/Cos (%)	C Water (%)	Y_1* GS (nm)	Y_2* PDI	Y_3* %T	Y_4* Viscosity (cp)
1	28.49	53.20	18.31	26.42±0.37	0.42±0.08	98.76±0.08	342.83±3.55
2	24.36	51.23	24.41	29.52±0.10	0.41±0.02	86.12±0.72	495.83±5.78
3	23.20	62.03	14.77	25.87±1.31	0.43±0.07	98.36±0.57	285.50±2.04
4	31.38	58.62	10.00	34.12±1.42	0.35±0.05	92.56±1.54	320.20±3.44
5	40.55	49.45	10.00	73.01±3.03	0.59±0.07	75.25±0.51	336.30±2.46
6	45.00	45.00	10.00	68.64±2.18	0.29±0.05	61.93±4.28	324.17±5.92
7	38.46	45.00	16.54	58.22±3.58	0.42±0.06	79.05±2.32	354.77±6.23
8	45.00	45.00	10.00	63.96±3.10	0.25±0.02	65.21±3.23	333.03±2.59
9	20.00	57.26	22.74	18.75±1.86	0.68±0.02	99.11±0.30	433.90±1.47
10	20.00	70.00	10.00	151.00±28.82	0.58±0.01	72.03±0.65	312.40±5.20
11	20.00	70.00	10.00	147.00±33.93	0.56±0.01	68.85±0.06	340.87±2.95
12	29.44	45.56	25.00	29.89±1.78	0.84±0.01	85.29±2.10	418.97±2.50
13	29.44	45.56	25.00	28.37±2.26	0.80±0.01	80.86±1.82	456.63±3.43
14	20.00	57.26	22.74	15.20±1.18	0.65±0.00	99.63±0.60	470.23±19.20
15	38.46	45.00	16.54	46.15±3.02	0.47±0.04	87.39±2.56	321.77±4.46
16	35.32	51.81	12.87	59.49±3.37	0.31±0.03	77.85±1.35	382.80±3.46

Notes: *All values are represented as mean ± standard deviation of three measurements for three different batches (n = 3). Collagen (10 mg) was incorporated in all formulations with a final concentration of 1% w/w.
Abbreviations: S/Cos, surfactant/cosurfactant; GS, globule size; PDI, polydispersity index; %T, percent transmittance.

In vitro Characterization of Collagen-Loaded NEs

Globule Size (GS) and Polydispersity Index (PDI) Determinations

The mean globule size (GS) and polydispersity index of the size distribution (PDI) for each NE were measured by photon correlation spectroscopy using the Malvern zeta-sizer (Ver.6.20, Malvern Instruments Ltd., Worcestershire, UK).[26] Analysis was performed at 25±2 °C and each reported value is the average of three measurements for three different batches.[27]

Optical Clarity

The optical clarity or the percent transmittance (%T) of NEs was measured via a UV-vis spectrophotometer (UV-1800; Shimadzu, Kyoto, Japan) at a wavelength of 600 nm.

Rheological Measurements

The rheological properties of NEs were determined via a cone-plate Brookfield Digital Rheometer Model DV-III (Brookfield Engineering LABS, Stoughton, MA) equipped with a flat spindle, type CP 40. The determination of the apparent viscosity measurements of NEs samples (1.5 g) was conducted at a variable spindle speed (0, 10, 15, 20, 30, 50, 70, 90, 100, and 120 rpm) within 90 seconds, and torque between 15.0% and 85.0%, at 25±2 °C. To compare the viscosity values of NEs between the dissimilar stresses, a 100 rpm as a spindle speed (after 30 seconds) was selected. The average ± standard deviation of three runs for three different batches was recorded.

Transmission Electron Microscopy (TEM) and pH Measurements

The inherent structure and topography of the optimized NE, containing either collagen or Vit C, were elucidated by Joel JEM 1230 transmission electron microscope (Tokyo, Japan), while their pH value was measured with a pH meter (Jenway, UK).[28]

Stability Studies

The thermodynamic stability of the optimized NE containing either collagen or Vit C was assessed by the protocol previously reported by Shafiq et al.[29,30] The optimized NEs were subjected to six heating-cooling cycles between the temperature of (4°C) and (45°C) for 48 h at each temperature and then centrifuged at 3500 rpm for 30 min. Finally, the optimized NEs were exposed to three freeze–thaw cycles between (−20°C) and (+25°C) for 48 h at each temperature. Moreover and according to ICH guidelines, the optimized NEs were stored in amber glass vials at 25±2 °C/60±5% RH for 6 months. At the end of the storage period, GS, PDI, %T, and viscosity were determined thrice and the results were compared to that attained from the freshly prepared NE, where the statistical significance was determined using GraphPad Prism Version 9 (San Diego, CA, USA), at $p < 0.05$.

In vitro Cellular Studies

Cell Culture

All in vitro cellular studies were performed at the Egyptian National Cancer Institute (Cairo, Egypt). Normal human fibroblast (HFB4) (PCS-201-010™) and Baby Hamster Kidney fibroblasts (BHK) (CCL-10™) cell lines were obtained commercially from the American Type Culture Collection (ATCC) (Manassas, USA). The cell lines were cultured and maintained in Roswell Park Memorial Institute-1640 (RPMI-1640) medium, which was charged with 10% fetal bovine serum, 1.5 g/L sodium bicarbonate, 2 mM L-glutamine, and 1% penicillin/streptomycin. The cells were kept at 37 °C in the prescence of 5% CO_2.

Cell Viability Assay

Sulforhodamine B (SRB) assay was used to investigate the cytotoxicity of the investigated treatments. In 96-well plates, exponentially growing cells were seeded at an initial density of 5×10^3/well and left in the incubator for 24 h. The considered treatment groups were Vit E, Vit C, collagen, plain NE lacking Vit E, plain NE, Vit C-loaded NE, collagen-loaded NE, and a mixture of collagen- and Vit C-loaded NEs (1:1). Different treatments with various concentrations ranging from 0 to 50 µL/mL were added to human HFB4 and BHK cell lines and incubated for 48 h at 37 °C to assess their effect on cell growth and survival. Trichloroacetic acid (10%) was used for cell fixation and left for 1 h at 4 °C,

while SRB (0.4%) was added to stain the cells. After 30 min, the cells were rinsed with acetic acid (1%) four times, then left to dry. Tris base (10 mM, pH 10.5) was added to dissolve the dye, then the optical density (O.D.) was measured spectrophotometrically at 570 nm via the microplate reader (Tecan SunriseTM, Switzerland). GraphPad InStat Software, version 7.01 (GraphPad, USA) was used to create sigmoidal dose–response curve-fitting models and to carry out the analysis of the data by applying a one-way analysis of variance (ANOVA) then Tukey multiple comparison post-hoc test. Results were considered statistically significant at $P < 0.05$.

Scratch Wound Healing Assay

HFB4 and BHK cells were cultured in six-well plates and then left for 24 h to form an adherent monolayer. This layer was then gently injured in a unidirectional way across the center of the well using a sterile pipette tip (1 mL). A gap distance equivalent to the external diameter of the pipette tip (0.5 mm) was produced and the elimination of the detached cells was completed by washing the wells with fresh medium twice. Different treatments (Vit E, Vit C, collagen, plain NE lacking Vit E, plain NE, Vit C-loaded NE, collagen-loaded NE, and a mixture of collagen and Vit C-loaded NEs (1:1)) were added at 50 µL/mL and the plates were incubated for 48 h. After washing the cells with phosphate buffer saline (PBS), they were fixed for 30 min with 3.7% paraformaldehyde. The cells were stained with crystal violet (1%) in 2% ethanol for 30 min. Micrographs of the stained monolayer were captured on a microscope and the gap distance was measured (when possible) by drawing lines through the edge of repopulating fibroblast cells and quantifying the cell-free distance remaining via the Leica Qwin-Plus software (Leica Microsystems, UK).

In vivo Studies

The procedures of the in vivo studies performed using male Wistar rats were pre-approved by the Research Ethics Committee in the Faculty of Pharmacy (REC-FOPCU), Cairo University (PI 2971) and were in compliance with the Guide for Care and Use of Laboratory Animals (NIH Publication No. 85-23, revised 2011). The animals (200–250 g) were maintained in a regulated environment of controlled temperature (23 ± 2 °C) and humidity (55±10%), and alternating light–dark cycles (12 h). The rats were nourished with a commercial chow and water (ad libitum).

Confocal Laser Scanning Microscopy (CLSM) Study

CLSM affords data about the shuttling of drugs by delivery systems through biological tissues. Rhodamine B dye (a hydrophilic fluorescent agent) was selected to mimic the behavior of water-soluble actives. The penetration and distribution of Rhodamine B dye in the skin layers after its topical application as an aqueous solution or loaded into the optimized NE were compared using CLSM. Before the experiment, the dorsal skin of six male Wistar rats was shaved and circumscribed, then the animals were allocated randomly into two groups (n=3). Group (A) received topical application of Rhodamine B dye aqueous solution, while group (B) was treated with Rhodamine B dye-loaded NE. After 8 h, the rats were decapitated and the skin samples were excised and washed with phosphate buffer saline (pH 7.4), then directly sandwiched between a glass slide and a coverslip, and finally inspected via CLSM.

In vivo Evaluation of the Optimized NE as a Protective Agent Against UVB Irradiation-Induced Skin Damage

Before the study, the dorsal hair was shaved by an electric clipper and specified areas were circumscribed. In total, 25 rats were separated randomly into 5 groups (n=5), where the calculation of the sample size was based on Mead's test.[31] Group (A): Control group; the rats did not receive any treatment and were not irradiated, group (B): Positive control group; the rats were UVB-irradiated and did not receive any treatment, group (C): Vit C-loaded NE-treated group; group (D): collagen-loaded NE-treated group, and group (E); Mixture of collagen and Vit C-loaded NEs (1:1)-treated group. The rats in groups (C), (D), and (E) received prophylactic topical treatment on the circumscribed dorsal skin with 0.5 g of Vit C-loaded NE, collagen-loaded NE, as well as collagen and Vit C-loaded NEs mixture (all at a concentration of 1% w/w), respectively, once daily for 1 week before starting the irradiation protocol, and 30 min before irradiation. For UV exposure, the rats were irradiated with a UVB lamp (290–320 nm), at a dose of 100 mJ/cm^2/day for 5 days, receiving a total dose of 500 mJ/cm^2. Three hours after the last exposure to UVB, the rats were euthanized by decapitation.[32] Specimens of dorsal skin were excised and fixed by immersion into 10% formalin. The dehydration of the specimens was performed with gradient series of alcohol then treated with xylene and finally

embedded in paraffin blocks. Five-micrometer thick sections were microtomed and stained with hematoxylin and eosin (H&E). Skin sections were inspected by light microscopy and photographed with a full HD microscopic camera operated by the Leica application module (Leica Microsystems GmbH, Wetzlar, Germany).

Results

Pseudo-Ternary Phase Diagram

According to the outcomes of the preliminary trials (data not shown), vitamin E and safflower oil (1:3) represented the oily phase, Span 80, and Kolliphor EL (1:1) were set as surfactants, while Arlasolve was used as a cosurfactant. As depicted in Figure 2, the pseudo-ternary phase diagram allows for distinguishing nanoemulsion (contoured) areas and emulsion regions. Consequently, and according to the NE area, defined percentages of the oils (20–45%), the surfactant/ cosurfactant (S/Cos) (45–70%), and water (10–25%) were selected (represented by the black triangle), which were further included as independent variables in a D-optimal mixture design.

Fitting of the Models

The Design Expert® software proposed 16 runs considering three independent variables: the percentage of oils (A), the percentage of S/Cos (B), and the percentage of water (C) with four experimental responses, namely (GS) (Y_1) in nm, (PDI) (Y_2), (%T) (Y_3), and viscosity (Y_4) in cp, as displayed in Table 1. The relationship between the dependent and independent variables was constructed as per the polynomial equations generated by the statistical analysis, where the cubic model was selected for the analysis of GS and PDI, whereas the quadratic model was selected for %T and the linear model for the viscosity, Table 2. The P values were found to be less than 0.05 which confirmed the significance of the model-fitting following the ANOVA, and this was accompanied by a non-significant lack of fit ($P > 0.05$). Remarkably, a model with an R^2 of more than 0.90 signifies a high correlation between the data.[33] A difference of less than 0.2 between the predicted and adjusted R^2 demonstrates the fitness of the nominated model to the data, which was detected in all the measured responses except PDI. The adequacy of precision that determines the ratio of signal to noise was quite higher than four which supported the adequacy of the signal in the selected model,[34] in addition, the chosen models showed the lowest PRESS values. The GS and PDI varied widely in the design space, with values of 15.20±1.18 to 151.00±28.82 nm, and 0.25±0.02 to 0.84±0.01, respectively, which infers the influence of the concentration of different ingredients on the GS and PDI. The %T ranged from 61.93±4.28 to 99.63±0.60%, while the viscosities of the developed systems were in the range of 285.50±2.04–495.83±5.78 cp suggesting suitability for topical application. The final equations in terms of actual components were as follows:

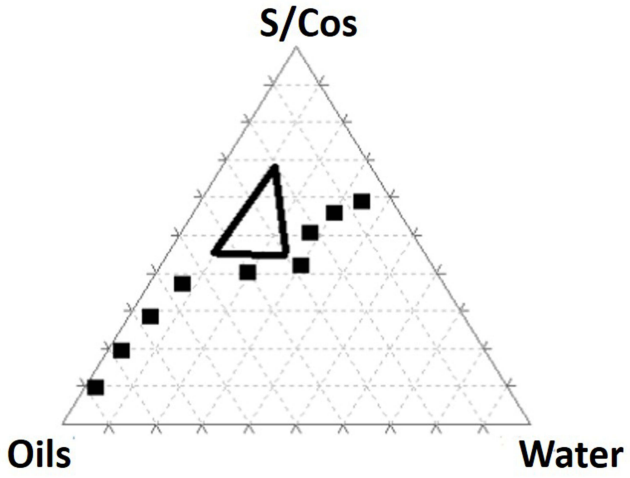

Figure 2 Pseudo-ternary diagram of vitamin E and safflower oil (1:3), Span 80/kolliphor EL/ Arlasolve (1:1:1), and water. The defined percentages of the oils (20–45%), the surfactant/ cosurfactant (S/Cos) (45–70%), and water (10–25%) are represented by the black triangle.

Table 2 Summary of Model Statistics for the Measured Responses

Response	Model	SD	R^2	Adjusted R^2	Predicted R^2	PRESS
Y_1: GS	Linear	29.67	0.5488	0.4794	0.2536	18,933.41
	Quadratic	16.80	0.8887	0.8331	0.7157	7212.14
	Cubic	4.07	0.9961	0.9902	0.9823	449.19
Y_2: PDI	Linear	0.14	0.4569	0.3734	0.1654	0.39
	Quadratic	0.13	0.6364	0.4546	0.2286	0.36
	Cubic	0.026	0.9915	0.9787	0.7273	0.13
Y_3: %T	Linear	10.02	0.4405	0.3544	0.1000	2100.27
	Quadratic	5.39	0.8755	0.8133	0.6779	751.64
	Cubic	3.26	0.9727	0.9318	0.3152	3069.33
Y_4: Viscosity	Linear	38.29	0.6911	0.6436	0.5711	26,470.12
	Quadratic	32.74	0.8264	0.7395	0.6138	23,830.24
	Cubic	21.63	0.9545	0.8863	1.6081	160,900

Note: The statistic values of the selected model for each response are underlined.
Abbreviations: SD, Standard deviation; GS, globule size; PDI, Polydispersity index; %T, Percent transmittance, PRESS, Predicted residual error sum of squares.

$$\begin{aligned} GS &= -79.57 * A + 37.48 * B + 150.18 * C + 0.81 * A * B - 3.31 * A * C - 3.06 * B * C + 0.07 \\ &\quad * A * B * C + 0.02 * A * B * (A - B) + 0.02 * A * C * (A - C) - 2.59x10^{-3} * B * C * (B - C) \end{aligned} \quad (1)$$

$$\begin{aligned} PDI &= -0.92 * A + 0.07 * B - 4.71 * C + 0.02 * A * B + 0.12 * A * C + 0.08 * B * C - 1.42x10^{-3} * A * B \\ &\quad * C + 1.83x10^{-4} * A * B * (A - B) - 6.08x10^{-4} * A * C * (A - C) - 2.43x10^{-4} * B * C * (B - C) \end{aligned} \quad (2)$$

$$\%\ T = -3.86 * A - 1.37 * B - 13.24 * C + 0.11 * A * B + 0.19 * A * C + 0.26 * B * C \quad (3)$$

$$Viscosit = 2.16 * A + 2.37 * B + 11.00 * C \quad (4)$$

It should be noted that the main variables ([A], [B], and [C]) signify the middling fallouts of fluctuating one variable at a time between its low to high value, and the interactions [A][B], [B][C], and [A][C] express how the responses alter when two or three factors vary simultaneously. Moreover, a positive sign preceding each term points to a synergistic consequence; however, a negative sign entitles an antagonistic outcome on the measured responses. Figure 3 represents the 3D surface plots demonstrating the effect of the independent variables, the percentage of oils (A), the percentage of S/Cos (B), and the percentage of water (C) on (I) globule size in nm (GS), (II) polydispersity index (PDI), (III) percent transmittance (%), and (IV) viscosity in cp.

Optimization of the Design

To establish the criteria for selecting the optimized formulation, minimum GS and PDI, and maximum %T and viscosity were set, and the software was allowed to predict the optimized NE. The predicted NE (with a desirability value of 0.808) was prepared with 25% oils, 54.635% S/Cos, and 20.365% water in triplicate, and the responses were measured. The optimized collagen-loaded NE showed GS of 19.41±4.17 nm with a PDI value of 0.50 ± 0.11, in addition, % T was 99.98 ±0.01%, and the measured viscosity was 402.00±5.02 cp. The practically obtained responses showed insignificant different results ($P < 0.05$) compared to the predicted values, Table 3. Moreover, the optimized NE was prepared and loaded with Vit C, which exhibited GS of 26.15±1.02 nm, PDI of 0.49±0.04, % T of 98.34±0.21%, and viscosity of 357.00±11.31 cp.

TEM and pH Measurements

The TEM micrographs of the optimized collagen-loaded NE and Vit C-loaded NE are exhibited in Figure 4. The micrographs revealed dispersed spherical water globules with a size comparable to those obtained from the zeta-sizer.

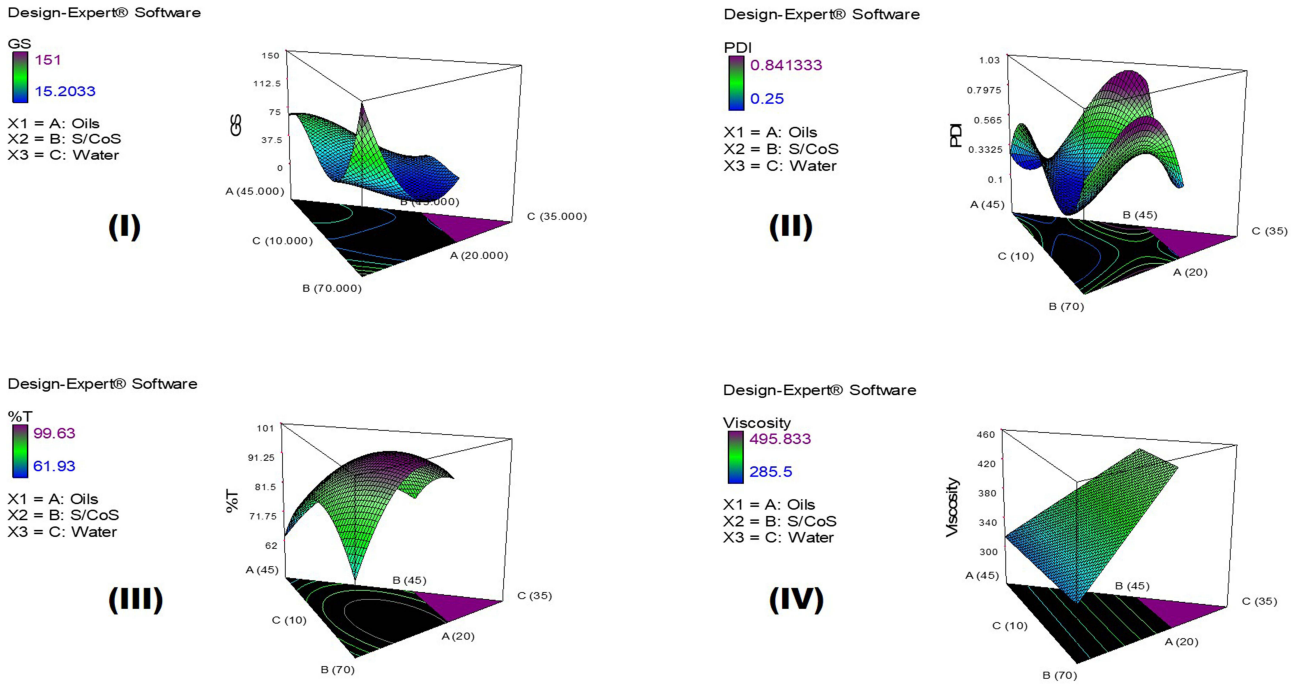

Figure 3 3D surface plots demonstrating the effect of the independent variables; the percentage of oils (A), the percentage of S/Cos (B), and the percentage of water (C) on (**I**) globule size in nm (GS), (**II**) Polydispersity index (PDI), (**III**) Percent transmittance (%), and (**IV**) Viscosity in cp.

The measured pH value of collagen-loaded NE was found to be 5.68, and the pH value of Vit C-loaded NE was found to be 4.30.

Stability Studies

After storage at 25±2 °C/60±5% RH for 6 months, the optimized collagen-loaded NE and Vit C-loaded NE continued to be transparent and clear lacking any precipitation or phase separation. The values of GS, PDI, %T, and viscosity were not altered significantly ($P > 0.05$), suggesting that the optimized NEs were stable under the above conditions (Table 4). Additionally, the physical stability of the optimized NEs was maintained without any phase separation or drug precipitation upon centrifugation at 3500 rpm for 30 min or exposure to repetitive extreme conditions of temperature through heating-cooling and freeze–thaw cycles.

Table 3 The Observed and the Predicted Values of the Optimized Collagen-Loaded NE

Factor	**Optimized Level (D=0.808)**		
A: Oils (%) B: S/Cos (%) C: Water (%)	25 54.635 20.365		
Response	**Expected**	**Observed#**	**Residual***
Y_1: GS (nm)	15.20	19.41±4.17	−4.21
Y_2: PDI	0.51	0.50 ± 0.11	−0.01
Y_3: %T	99.63	99.98±0.01	−0.35
Y_4: Viscosity (cp)	407.89	402.00±5.02	4.11

Notes: *Residual = expected value – observed value. #Mean ± Standard deviation (n = 3).
Abbreviations: D, desirability value; S/Cos, surfactant/cosurfactant; GS, globule size; PDI, polydispersity index; %T, percent transmittance.

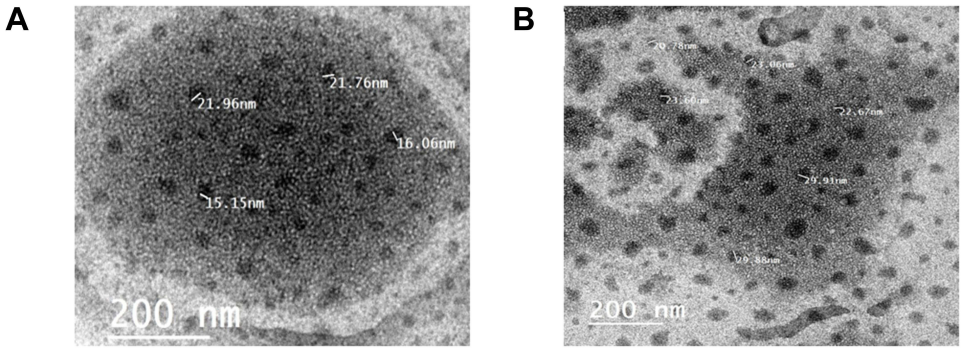

Figure 4 TEM micrographs of (**A**) collagen-loaded NE, and (**B**) Vit C-loaded NE.

In vitro Cellular Studies

Cell Viability and Proliferation

In this study, the influence of the different treatments on cell viability was evaluated on the HFB4 and BHK cell lines as shown in Figure 5A and Figure 5B, respectively. After 48 hours of treatment, NE loaded with Vit C, collagen, or a mixture of both increased the cell proliferation and enhanced the surviving fraction of both cell lines significantly ($P < 0.05$) compared to the untreated cells or cells treated with either collagen or Vit C solutions or Vit E. The mixture of collagen and Vit C-loaded NEs produced the highest increase in cell survival at all concentrations that ranged from 0 to 50 µL/mL. As displayed in Figure 5C and D, at 50 µL/mL as the highest concentration, collagen and Vit C-loaded NEs mixture resulted in a 1.18- and 1.21-fold increase in cell survival in HFB4 and BHK cell lines, respectively. This increase was statistically significant ($P < 0.05$) compared to those observed with NEs containing the solo drugs. Vit C- or collagen-loaded NEs also produced a statistically significant elevation ($P < 0.05$) in cell survival compared to their solutions.

Wound Healing Study

This experiment aimed to evaluate the effect of the different treatments on wound healing and cell migration in the HFB4 and BHK cells as shown in Figure 6. As shown in Figure 6A, the gap distance (0.5 mm) produced by the pipette tip was obvious at zero time and decreased to approximately 0.15–0.2 mm after 48 h without treatment (Figure 6B). This gap was filled to a certain extent with proliferated cells in the wells treated with Vit E, Vit C, collagen, plain NE lacking Vit E, and plain NE (Figure 6C–G, respectively). Treatment with Vit C (Figure 6H) or collagen-loaded NE (Figure 6I) resulted in healing to a greater extent compared to their drug solutions, which could be demonstrated by the presence of more regenerated cells in the gap. The gap distance in the HFB4 and BHK cell lines reached a complete closure with collagen- and Vit-C-loaded NE mixture (Figure 6J), which indicates a synergistic effect.

In vivo Studies

Confocal Microscopy

To envision the influence of the formulation (NE) on drug shuttling through the skin following topical application, the penetration and diffusion of Rhodamine B dye from the optimized NE and its solution (as a control) in the skin layers

Table 4 Characteristics of the Optimized Collagen-Loaded NE and Vit C-Loaded NE Before and After Storage at (25±2 °C/60±5% RH) for 6 Months

Formulations	GS (nm)	PDI	T (%)	Viscosity (cp)
Collagen-loaded NE before storage	19.41±4.17	0.50 ± 0.01	99.98±0.01	402.00±5.02
Collagen-loaded NE after storage	19.95 ± 3.37	0.51± 0.1	99.98± 0.12	411.00±9.31
Vit C-loaded NE before storage	26.15 ± 1.02	0.49±0.04	98.34±0.21	357.00±11.31
Vit C-loaded NE after storage	25.82 ± 2.35	0.52±0.03	98.57±0.11	365.00±8.78

Abbreviations: GS, globule size; PDI, polydispersity index; %T, percent transmittance.

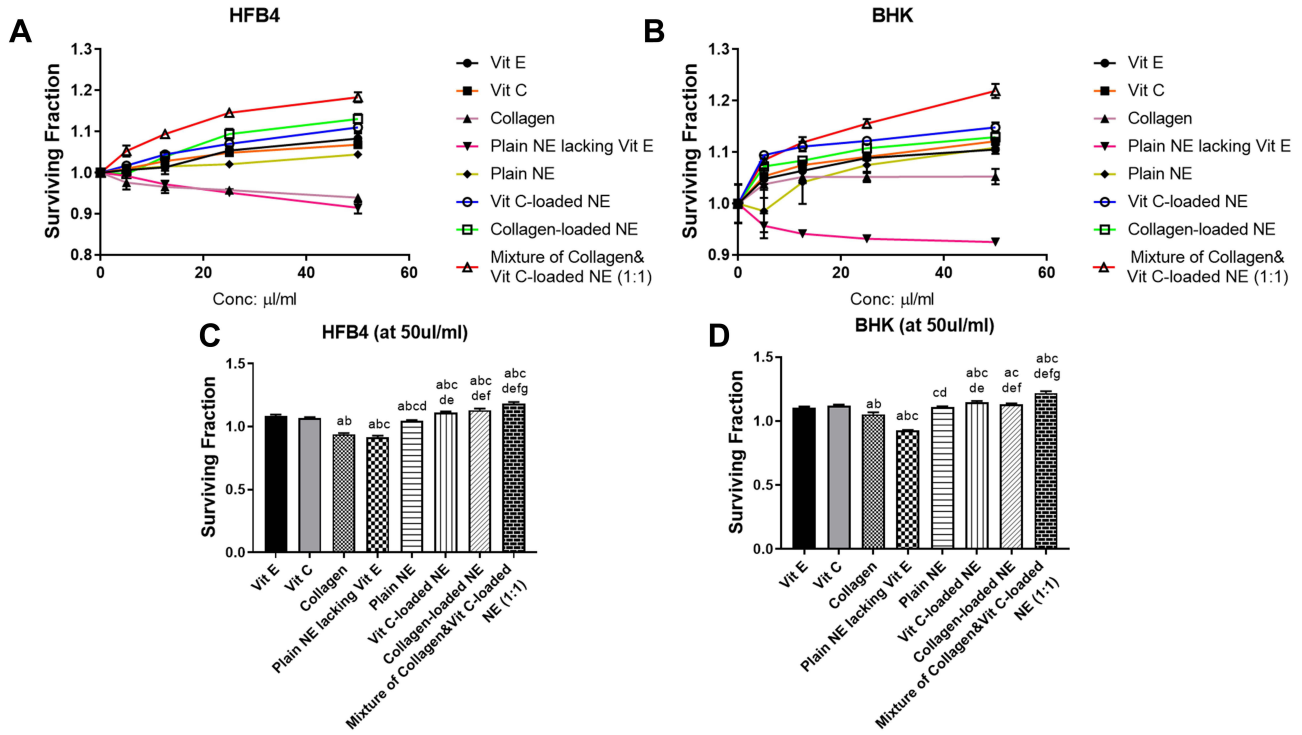

Figure 5 Surviving fraction after applying the different treatments (Vit E, Vit C, collagen, plain NE lacking Vit E, Plain NE, Vit C-loaded NE, collagen-loaded NE, and a mixture of collagen and Vit C-loaded NEs) for 48 h on (**A**) HFB4 cells, (**B**) BHK cells, (**C**) HFB4 cells after applying the treatments at the highest concentration (50 µL/mL), and (**D**) BHK cells after applying the treatments at the highest concentration (50 µL/mL). The actual data represent the mean ± SD of three separate experiments performed in duplicates. Results were analyzed for statistical significance by one-way analysis of variance (ANOVA) followed by Tukey multiple comparison post-hoc test. [a]Significant difference from Vit E, [b]Significant difference from Vit C, [c]Significant difference from collagen, [d]Significant difference from Plain NE lacking Vit E, [e]Significant difference from Plain NE, [f]Significant difference from Vit C-loaded NE, and [g]Significant difference from collagen-loaded NE ($p<0.05$).

were observed via CLSM. Figure 7 illustrates rhodamine B retention in the stratum corneum layer when introduced to the skin in its aqueous solution (Figure 7A), whereas the dye was permeated through the skin layers at the depth of up to 260 µm after the topical application of the optimized NE (Figure 7B). Moreover, the dye was represented with a weak fluorescence in the specimens treated with the dye aqueous solution, while higher fluorescence intensities were observed in the case of NE.

In vivo Protection Against UVB Irradiation-Induced Skin Damage

Figure 8 demonstrates the histopathological observations of untreated denuded rat skin, UVB-irradiated rat skin, and UVB-irradiated rat skin pretreated with Vit C-loaded NE, collagen-loaded NE, and a mixture of collagen and Vit C-loaded NEs. The histological examination of the control group (1) revealed normal epidermal and dermal layers along with normal structure of different skin appendages, including hair follicles, sebaceous glands, and sweat glands (Figure 8A). The shaved rat skin exposed to UVB irradiation displayed alterations mainly in the epidermis, where hyperkeratosis was frequently observed in many sections, and acanthosis was manifested by thickening in the epidermal layer. The epidermis contained numerous shrunken cells known as sunburn cells near the basal cell layer, as demonstrated by arrows in Figure 8B. Topical treatment with Vit C-loaded NE and collagen-loaded NE showed better skin shape and less roughness owing to their healing effects (Figure 8C and D, respectively). However, the effect of collagen and Vit C-loaded NEs mixture was more pronounced compared to Vit C-loaded NE or collagen-loaded NE, where NE containing both drugs reduced the skin damage to an extent that the skin was free from any detectable alterations (Figure 8E).

Discussion

Nanoemulsions consist of water, oil, and surfactant, so these systems can be represented by ternary diagrams; and since a co-surfactant is incorporated in the systems, pseudo-ternary diagrams are used. A co-emulsifier is usually added to

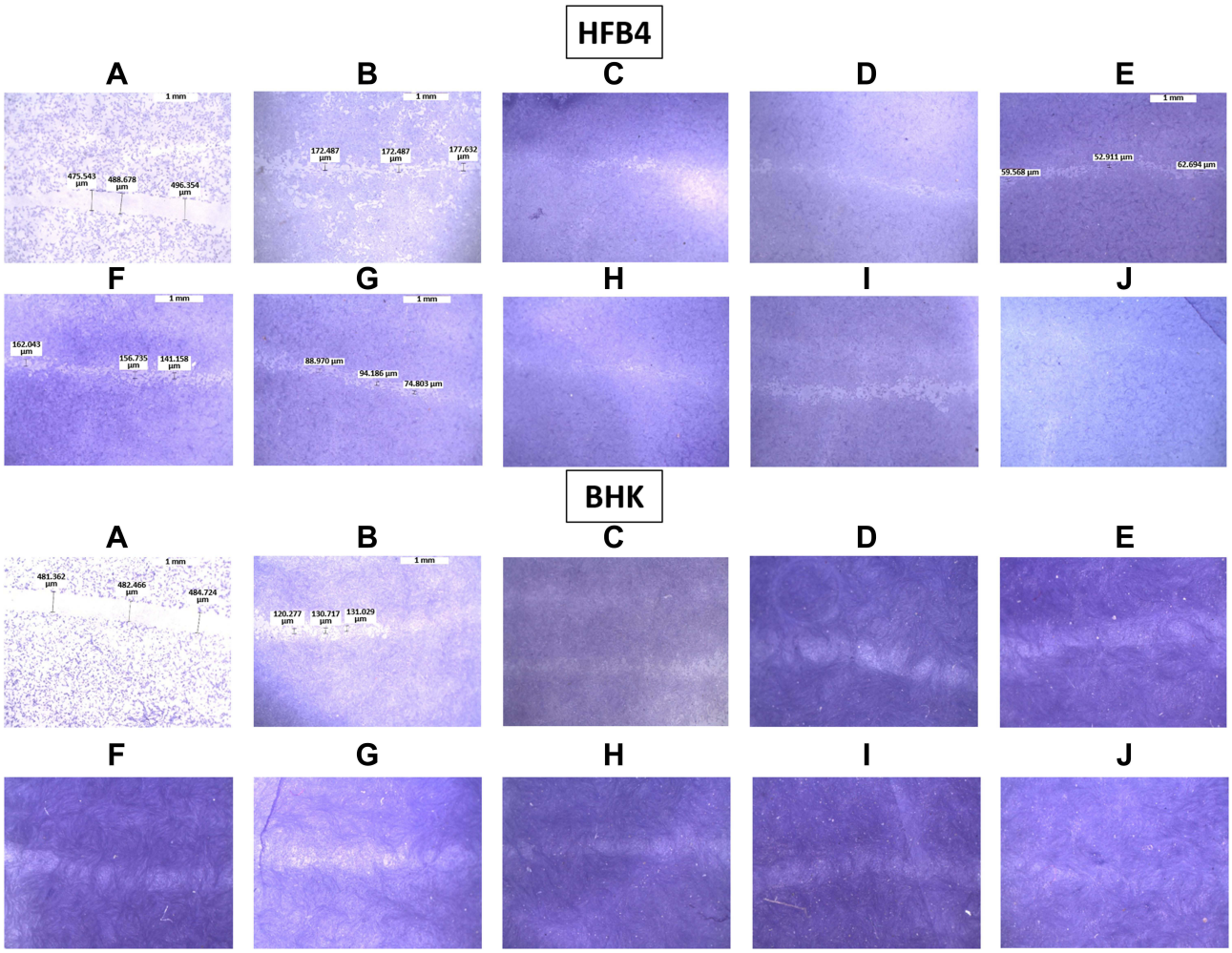

Figure 6 Micrographs of the stained healed monolayer of HFB4 and BHK cells. (**A**) Control at 0 h, (**B**) control after 48 h, (**C**) Vit E, (**D**) Vit C, (**E**) collagen, (**F**) plain NE lacking Vit E, (**G**) plain NE, (**H**) Vit C-loaded NE, (**I**) collagen-loaded NE, and (**J**) A mixture of collagen- and Vit C-loaded NEs.

advance the system's stability.[35] As for the oily phase, an optimum composition is required to form stable NEs. The inclusion of Vit E in such formulation was optimum as per its structural features, where the presence of the hydroxyl group allowed the system to incorporate more amounts of water compared to those formulated using safflower oil solely. Also, it can donate a hydrogen atom to reduce free radicals and thus enhancing the system's stability. Moreover, the hydrophobic side chain of Vit E permits boosted penetration into biological membranes.[36] The choice of the surfactants is also critical and this selection was based on their solubility and miscibility with the oils, taking into consideration that the used non-ionic surfactants are considered to be less toxic than their ionic counterparts. The surfactant mixture of Span 80 and Kolliphor EL was reported earlier to work synergistically to reduce the water–oil interfacial tension to an extent more than that produced by each of them. Previously during the preparation of NE, it was stated that the adsorption and arrangement of Span 80 molecules on the oil-water interfacial boundary are easier in the presence of Kolliphor EL as the mixture boosts the dispersion and the solubilization of the internal phase into sub-micrometer droplet size.[14] The selection of Arlasolve as a co-surfactant was based on its miscibility with the selected oils and surfactants, besides its ability to enhance the delivery of actives through being incorporated in many cosmeceutical preparations.

As mentioned earlier and as per the results of model fitting, the cubic model was selected for the analysis of GS and PDI, whereas the quadratic model was selected for %T and the linear model for the viscosity. The GS of NE ought to be as small as possible so that their penetration into the deeper layers of the skin is facilitated to deposit collagen. As per the 3D surface plot of GS (Figure 3I) and ANOVA results, the oil and S/Cos proportions interaction (AB) and the oil, S/Cos,

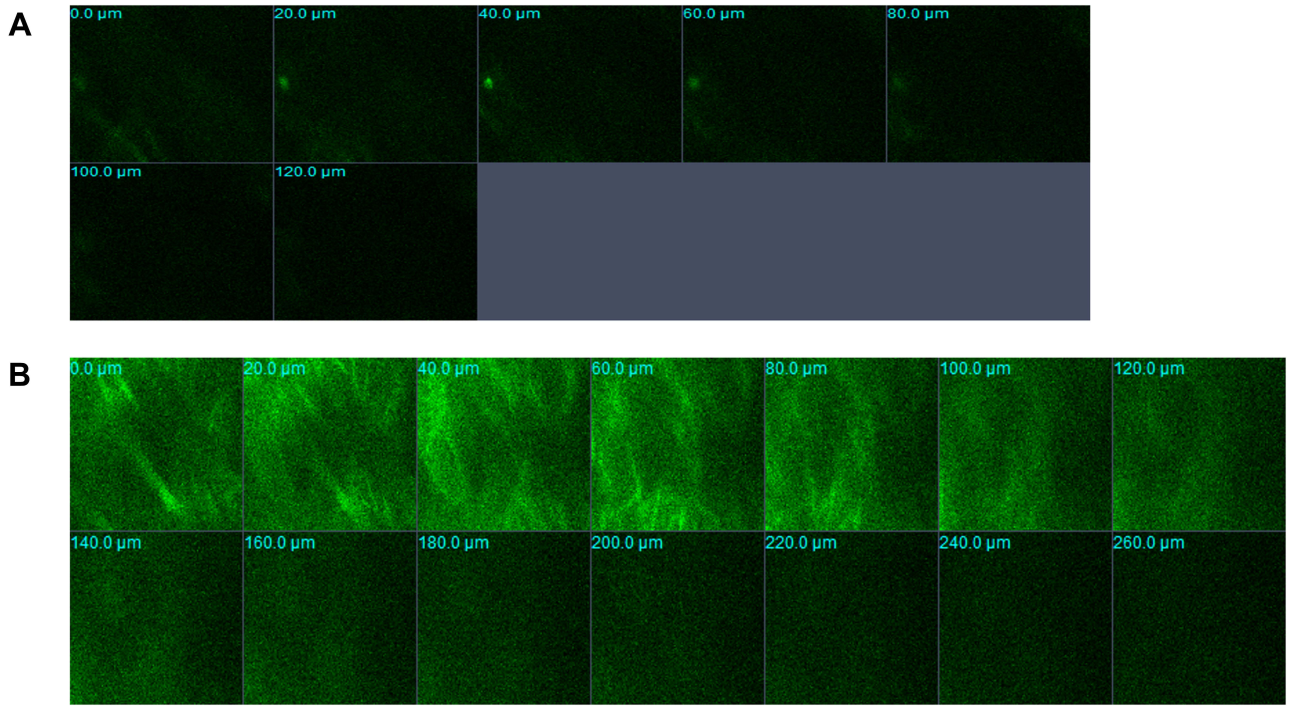

Figure 7 CLSM micrographs of (**A**) Rhodamine B dye aqueous solution and (**B**) Rhodamine B dye-loaded NE.

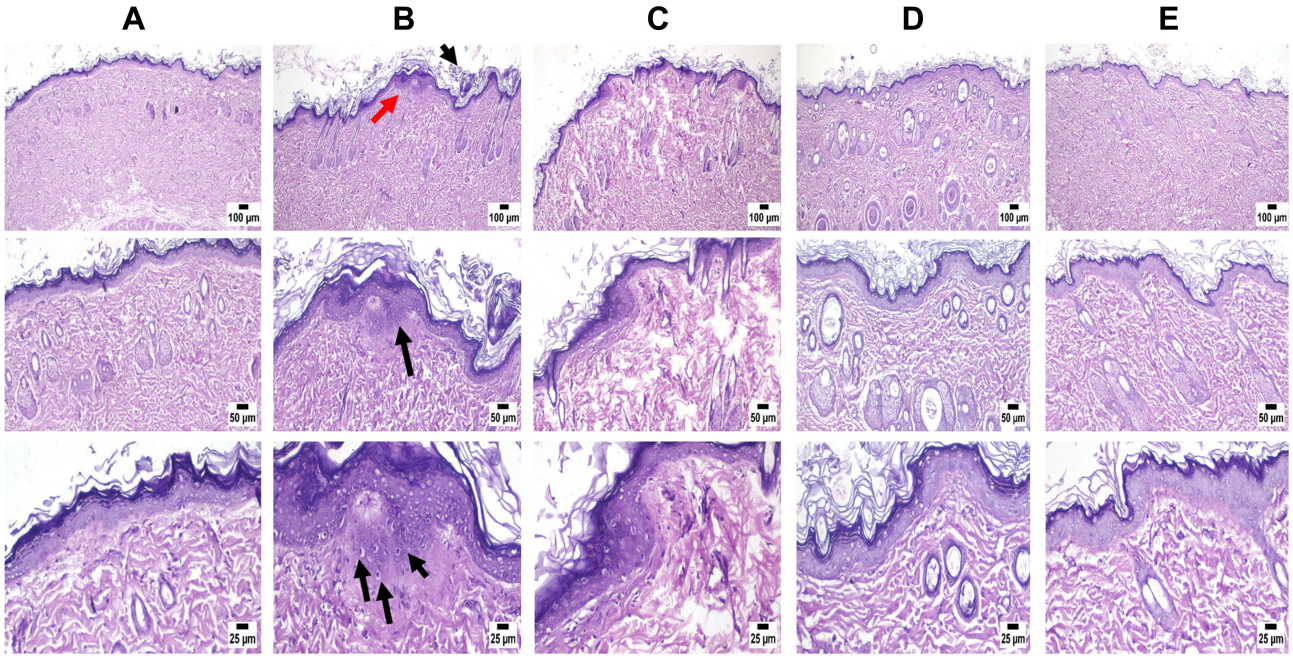

Figure 8 Microscopic examination of skin samples from (**A**) control group revealing normal histology of skin, (**B**) positive control showing histopathological alterations mainly in the epidermis. Hyperkeratosis and acanthosis (black arrows) are manifested by thickening in the epidermal layer (red arrow). The epidermis contained numerous shrunken cells known as sunburn cells near the basal cell layer (3 black arrows), (**C**) Vit C-loaded NE showing apparently normal skin with mild inflammatory cells infiltration, (**D**) collagen-loaded NE showing apparently normal skin, and (**E**) a mixture of collagen and Vit C-loaded NEs revealing skin free from any detectable alterations.

and water proportions interaction (ABC) showed a significant impact on GS ($P < 0.05$). According to equation (1), the oil proportion showed an antagonistic effect on the GS of NE, which could be explained in light of the fact that the higher percentages of oil, as an external phase of the W/O NE, minimized the probability of water droplets aggregations owing

to the dilution effect. In addition, more oil proportions increased the viscosity of the medium, and thus restricted the migration of water droplets.[37,38] Taking into consideration the significant oil and S/Cos proportions interaction (AB) and the oil, S/Cos proportions, and water interaction (ABC), higher proportions of oils when accompanied by small amounts of S/Cos yielded large GS, and this could be due to the adsorption of an insufficient number of S/Cos molecules at the interface. On the contrary, increasing the proportion of S/Cos and water, as an inner phase of the W/O NE, resulted in a decrease in GS, which is attributed to the lower possibility of water droplets coalescence due to the sufficiency of S/Cos molecules adsorption at the interface, and probably because of certain surface activity of collagen which was comfortably soluble in an increased proportion of inner water phase.[39] The largest GS (Run 10 and 11) was observed with the highest amount of S/Cos, and a possible explanation is that a highly viscous liquid crystalline phase could be formed which interfered with the spontaneous collapse of the water–oil interface in the NE.[40] Shakeel and Ramadan reported earlier that upon increasing the ratio of S/Cos to water, the droplet size significantly increases.[41] PDI is a dimensionless parameter that measures the breadth of size distribution considered from the cumulant analysis, with values from zero to one. According to the 3D surface plot of PDI (Figure 3II) and ANOVA results, the oil and water proportions interaction (AC), S/Cos and water proportions interaction (BC), and the oil, S/Cos, and water proportions interaction (ABC) showed a substantial influence on PDI ($P < 0.05$). As per equation (2), and regarding the oil and water proportions interaction (AC), PDI decreased with increasing oil proportion and decreasing water content as per the dilution effect of the external oily phase. Vis-à-vis, S/Cos and water proportions interaction (BC), where decreasing both S/Cos and water proportions decreased PDI values while increasing one of them or both resulted in the formation of systems with higher PDI values. This could be due to possible formulation instability caused by higher S/Cos proportion and hence give a chance for globule coalescence; known as Ostwald ripening.[42,43] Higher water content with lower S/Cos proportions led to the formulation of NE with a high PDI value, and this could be accredited to the inability of S/Cos to emulsify the inner aqueous phase in the outer oily one, where coalescence of the inner phase occurred. The 3D surface plot of %T (Figure 3III) and ANOVA results showed that the oil and S/Cos proportions interaction (AB), the oil and water proportions interaction (AC), and S/Cos and water proportions interaction (BC) significantly affected %T ($P < 0.05$). According to equation (3), decreasing the proportions of all components led to an increase in %T, while different combinations of the components showed a positive effect on %T. This could be explained by the fact that the formulation of NE requires an optimum combination of all components, and varying the proportion of any of them would alter the overall equilibrium of the system, which is mandatory to keep the drug at its ideal solubility level.[44] This fact is highly related to the physical properties of the surfactant-oil-water mixtures, which are dynamic and variable over time and space upon mingling of the organic phase with the aqueous phase.[45] It should be noted that the results of %T are in good harmony with that of GS, where NEs with smaller GS displayed a high %T. All NEs showed acceptable viscosity values as a topically applied dosage form; whereupon their application on the skin, this viscosity helps in retaining the actives for a suitable period of time, which guarantees better drug permeation and absorption. The viscosity of the NE is known to be a function of its components and their concentrations.[46] Moreover, viscosity analysis is crucial in explaining the interactions between the dispersed phase droplets and the continuous phase.[47] According to equation (4) and the 3D surface plot of the viscosity displayed in Figure 3IV, the viscosity of NEs was found to be directly related to the concentrations of all of its components. Higher viscosity values were observed with the formulated systems due to the inherent high viscosities of the oils, surfactants and cosurfactant, in addition to the oily nature of the external phase of W/O NE.

Based on the design analysis, the optimum formulation was elected and furtherly characterized for morphology, pH, and stability. The distinct spherical droplets observed with the TEM revealed the dispersion of water globules, which is attributed to the presence of a monolayer of S/Cos around each globule that acts as a barrier against globules coalescence leading to the formulation of a stable system.[48] In addition, no precipitation of the drug was observed which would affect the system stability.[49] As per the results of the stability study, the high stability observed with the formulated NEs is attributed to the plasticity of the interfacial film, which was maintained throughout the shelf life of NE and hindered phase separation.[50] The measured pH values of the formulated NEs were found to be appropriate for skin topical application.[24] In addition, the slightly acidic pH value observed with Vit C-loaded NE is preferable to enhance the stability of Vit C.[11]

Relating to the results of the in vitro cellular studies, it could be observed that the formulation played a profound role in enhancing the permeation of the actives, which in turn led to a significantly improved cell proliferation and an enhanced surviving fraction of HFB4 and BHK cell lines, in addition to the wound healing effect, especially when collagen and Vit C were applied together. This could be attributed to the process of tissue repair which involves a series of cellular events that include cell migration and the secretion of several mediators.[51] Previous studies highlighted the importance of collagen in tissue regeneration, where applying collagen or chemicals that increase its endogenous release to cutaneous skin lesions has shown an enhancement in cell migration and wound healing.[52,53] Based on this fact, several collagen-based formulations and matrices were proved to be very effective in halting the skin aging process due to collagen deficiency in fibroblast cultures.[54–56] Similarly, different studies have reported that Vit C plays a pivotal role in decelerating the aging process either through its direct effects or indirectly through increasing collagen synthesis,[57–60] as well as, acting by itself as a promoter of tissue repair.[61,62] Shibuya et al demonstrated an additive effect on aging-related skin atrophy when collagen and Vit C were administered together.[63] Also, Vit E was found to have cell protectant and antioxidant properties, which sustain the structural and functional integrity of the cellular membrane, besides being a free radical scavenger so averting the peroxidation of membrane fatty acids.[64] The results of the CLSM study came to prove the boosted permeability and retention of the formulated NE. This could be accredited to the nanoemulsion penetration-enhancing potentiality and its ability to advance the transport of drugs throughout the skin, via disturbing the lipid barrier of the stratum corneum, enriching skin hydration, and empowering the drive of drugs through the skin.[65]

As per the results of the in vivo study, it was pragmatic that the UVB irradiation caused some alterations in the skin principally in the epidermis. It is widely recognized that excessive contact with pollutants or long exposure to UV radiation results in skin aging with wrinkle formation due to loss of collagen.[66] Moreover, some studies revealed the skin changes implicated with UVB exposure, where hyperkeratosis and acanthosis are among the common alterations in skin morphology after irradiation.[67,68] Another important factor that causes skin damage is the oxidative stress that depletes vitamin C levels in the skin,[39,40] which is known to stimulate collagen synthesis and protect against UV-induced photodamage. According to the results, the group that was treated with collagen- and Vit C-loaded NEs mixture showed the most healthy skin features, as collagen was found to elevate the degree of hydration at the inner layers of the skin through the topical treatment with cosmetic formulations containing collagen peptides,[69] and boost the smoothness and the luminosity of the skin surface at the microtextural level.[3] Besides, Vit E (as a component of NE) and Vit C are famous for their skin protectant and topical antioxidants characteristics,[70,71] where applying the three ingredients led to the superlative results.

Conclusion

Skin delivery of collagen and prophylactic antioxidant therapy (including Vit C and Vit E) through a W/O nanoemulsion has been introduced to lessen UV-induced skin injury. In this study, a novel system was formulated using a mixture of safflower oil and Vit E as the oily phase, while Span 80 and Kolliphor EL were incorporated as a surfactant, and Arlasolve was employed as a cosurfactant for the first time. The optimized nanoemulsion, either loaded with collagen or Vit C, displayed a small globule size with spherical morphology, a high optical clarity, a topically accepted viscosity, and pH, as well as a good physical stability. The confocal laser scanning microscopy study proved the boosted permeability and retention of the formulated W/O nanoemulsion. The optimized NE loaded with collagen or Vit C, or the mixture of collagen and Vit C-loaded NEs revealed improved cell viability and enhanced wound healing properties on fibroblast cell lines (HFB4) and (BHK) compared to the actives' solutions. In addition, an in vivo study and histopathological investigations proved the efficacy of the developed system in shielding the skin against UV damage. In conclusion, the formulated NE containing skin protectant actives, namely collagen, Vit C, and Vit E, could be a promising ameliorative cosmeceutical preparation for skin protection against harmful UVB irradiation. Further investigations to compare the efficacy and long-term safety of the formulated NEs to commercial products, as well as clinical studies are considered.

Disclosure

The authors report no conflicts of interest in relation to this work.

References

1. Lokes K, Avetikov D, Stavitsky S, Rozkolupa O, Lutsenko N. The features of the face skin construction that influence on the formation of cicatricial tissues during sugical interventions. *Ukrain Dent Almanac*. 2019;(4):19–23. doi:10.31718/2409-0255.4.2019.03
2. Chung JH, Seo JY, Choi HR, et al. Modulation of skin collagen metabolism in aged and photoaged human skin in vivo. *J Investig Dermatol*. 2001;117(5):1218–1224. doi:10.1046/j.0022-202x.2001.01544.x
3. Aguirre-Cruz G, León-López A, Cruz-Gómez V, Jiménez-Alvarado R, Aguirre-álvarez G. Collagen hydrolysates for skin protection: oral administration and topical formulation. *Antioxidants*. 2020;9(2):181.
4. Avila Rodríguez MI, Rodriguez Barroso LG, Sánchez ML. Collagen: a review on its sources and potential cosmetic applications. *J Cosmet Dermatol*. 2018;17(1):20–26.
5. Mohania D, Chandel S, Kumar P, et al. Ultraviolet radiations: skin defense-damage mechanism. *Ultraviolet Light Human Health Dis Environ*. 2017;2017:71–87.
6. Kawashima S, Funakoshi T, Sato Y, et al. Protective effect of pre-and post-vitamin C treatments on UVB-irradiation-induced skin damage. *Sci Rep*. 2018;8(1):1–12.
7. Al-Niaimi F, Chiang NYZ. Topical vitamin C and the skin: mechanisms of action and clinical applications. *J Clin Aesthet Dermatol*. 2017;10(7):14.
8. Darr D, Combs S, Dunston S, Manning T, Pinnell S. Topical vitamin C protects porcine skin from ultraviolet radiation-induced damage. *Br J Dermatol*. 1992;127(3):247–253.
9. Ahmed IA, Mikail MA, Zamakshshari N, Abdullah A-SH. Natural anti-aging skincare: role and potential. *Biogerontology*. 2020;21(3):293–310.
10. Telang PS. Vitamin C in dermatology. *Indian Dermatol Online J*. 2013;4(2):143. doi:10.4103/2229-5178.110593
11. Elhabak M, Ibrahim S, Abouelatta SM. Topical delivery of l-ascorbic acid spanlastics for stability enhancement and treatment of UVB induced damaged skin. *Drug Deliv*. 2021;28(1):445–453. doi:10.1080/10717544.2021.1886377
12. Bora NS, Mazumder B, Mandal S, et al. Amelioration of UV radiation-induced photoaging by a combinational sunscreen formulation via aversion of oxidative collagen degradation and promotion of TGF-β-Smad-mediated collagen production. *Eur J Pharma Sci*. 2019;127:261–275. doi:10.1016/j.ejps.2018.11.004
13. Santander RG, Arriba MP, Cuadrado GM, Martinez MG-S, de la Rosa MM. Effects of "in situ" vitamin E on fibroblast differentiation and on collagen fibril development in the regenerating tendon. *Int J Dev Biol*. 2001;40(S1):S181–S182.
14. Ishak KA, Fadzil MFA, Annuar MSM. Phase inversion emulsification of different vegetable oils using surfactant mixture of cremophor EL and lipase-synthesized glucose monooleate. *LWT*. 2021;138:110568. doi:10.1016/j.lwt.2020.110568
15. Debnath S, Satayanarayana KV, Kumar GV. Nanoemulsion—a method to improve the solubility of lipophilic drugs. *Pharmanest*. 2011;2(2–3):72–83.
16. Chime S, Kenechukwu F, Attama A. Nanoemulsions—advances in formulation, characterization and applications in drug delivery. *Appl Nanotechnol Drug Deliv*. 2014;3:77–126.
17. Yousry C, Zikry PM, Basalious EB, El-Gazayerly ON. Self-nanoemulsifying system optimization for higher terconazole solubilization and non-irritant ocular administration. *Adv Pharm Bull*. 2020;10(3):389. doi:10.34172/apb.2020.047
18. Shukla T, Upmanyu N, Agrawal M, Saraf S, Saraf S, Alexander A. Biomedical applications of microemulsion through dermal and transdermal route. *Biomed Pharmacother*. 2018;108:1477–1494. doi:10.1016/j.biopha.2018.10.021
19. Praça FG, Viegas JSR, Peh HY, Garbin TN, Medina WSG, Bentley MV. Microemulsion co-delivering vitamin A and vitamin E as a new platform for topical treatment of acute skin inflammation. *Mater Sci Eng C*. 2020;110:110639. doi:10.1016/j.msec.2020.110639
20. Kumar N. D-optimal experimental approach for designing topical microemulsion of itraconazole: characterization and evaluation of antifungal efficacy against a standardized Tinea pedis infection model in Wistar rats. *Eur J Pharma Sci*. 2015;67:97–112. doi:10.1016/j.ejps.2014.10.014
21. Sionkowska A, Adamiak K, Musiał K, Gadomska M. Collagen based materials in cosmetic applications: a review. *Materials*. 2020;13(19):4217. doi:10.3390/ma13194217
22. Hasani-Javanmardi M, Fallah AA, Abbasvali M. Effect of safflower oil nanoemulsion and cumin essential oil combined with oxygen absorber packaging on the quality and shelf-life of refrigerated lamb loins. *LWT*. 2021;147:111557. doi:10.1016/j.lwt.2021.111557
23. Lin T-K, Zhong L, Santiago JL. Anti-inflammatory and skin barrier repair effects of topical application of some plant oils. *Int J Mol Sci*. 2015;19(1):70. doi:10.3390/ijms19010070
24. Abd-Elsalam WH, Ibrahim RR. Span 80/TPGS modified lipid-coated chitosan nanocomplexes of Acyclovir as a topical delivery system for viral skin infections. *Int J Pharm*. 2021;609:121214. doi:10.1016/j.ijpharm.2021.121214
25. Zeng L, Xin X, Zhang Y. Development and characterization of promising Cremophor EL-stabilized o/w nanoemulsions containing short-chain alcohols as a cosurfactant. *RSC Adv*. 2017;7(32):19815–19827.
26. Farag DB, Yousry C, Al-Mahallawi AM, El-Askary HI, Meselhy MR, AbuBakr N. The efficacy of Origanum majorana nanocubosomal systems in ameliorating submandibular salivary gland alterations in streptozotocin-induced diabetic rats. *Drug Deliv*. 2022;29(1):62–74.
27. Abd-Elsalam WH, Saber MM, Abouelatta SM. Trehalosomes: colon targeting trehalose-based green nanocarriers for the maintenance of remission in inflammatory bowel diseases. *Eur J Pharma Biopharma*. 2021;166:182–193.
28. Abd-Elsalam WH, Nagy YI, Abouelatta SM. Tailoring thixotropic mixed-lipid nanoconstructs of voriconazole for the management of Vulvovaginal candidiasis: formulation, statistical optimization, in vitro characterization and in vivo assessment. *Drug Deliv*. 2021;28(1):1877–1889.
29. Shafiq S, Shakeel F, Talegaonkar S, Ahmad FJ, Khar RK, Ali M. Development and bioavailability assessment of ramipril nanoemulsion formulation. *Eur J Pharma Biopharma*. 2007;66(2):227–243.
30. Tayel SA, El-Nabarawi MA, Tadros MI, Abd-Elsalam WH. Promising ion-sensitive in situ ocular nanoemulsion gels of terbinafine hydrochloride: design, in vitro characterization and in vivo estimation of the ocular irritation and drug pharmacokinetics in the aqueous humor of rabbits. *Int J Pharm*. 2013;443(1–2):293–305.
31. Kirkwood J, Hubrecht RC. *The UFAW Handbook on the Care and Management of Laboratory and Other Research Animals*. John Wiley & Sons; 2010.
32. Sharma MR, Mitrani R, Werth VP. Effect of TNFα blockade on UVB-induced inflammatory cell migration and collagen loss in mice. *J Photochem Photobiol B*. 2020;213:112072.

33. Arbain NH, Salim N, Masoumi HRF, Wong TW, Basri M, Rahman MBA. In vitro evaluation of the inhalable quercetin loaded nanoemulsion for pulmonary delivery. *Drug Deliv Transl Res*. 2019;9(2):497–507.
34. Todosijević MN, Cekić ND, Savić MM, Gašperlin M, Ranđelović DV, Savić SD. Sucrose ester-based biocompatible microemulsions as vehicles for aceclofenac as a model drug: formulation approach using D-optimal mixture design. *Colloid Polym Sci*. 2014;292(12):3061–3076.
35. Perez-Roman I, Garcia-Rodriguez JJ, Kiekens F, Cordoba-Diaz D, Cordoba-Diaz M. Enhanced nematocidal activity of a novel Artemisia extract formulated as a microemulsion. *Nat Prod Commun*. 2019;14(6):1–6.
36. Waseem A, Rishi L, Yaqoob M, Nabi A. Flow-injection determination of retinol and tocopherol in pharmaceuticals with acidic potassium permanganate chemiluminescence. *Analytical Sci*. 2009;25(3):407–412.
37. Bajpai A. Facile preparation of ionotropically crosslinked chitosan-alginate nanosorbents by water-in-oil (W/O) microemulsion technique: optimization and study of arsenic (V) removal. *J Water Process Eng*. 2019;32:100920.
38. Raviadaran R, Ng MH, Manickam S, Chandran D. Ultrasound-assisted water-in-palm oil nano-emulsion: influence of polyglycerol polyricinoleate and NaCl on its stability. *Ultrason Sonochem*. 2019;52:353–363.
39. Kupper S, Kłosowska-Chomiczewska I, Szumała P. Collagen and hyaluronic acid hydrogel in water-in-oil microemulsion delivery systems. *Carbohydr Polym*. 2017;175:347–354.
40. Wang L, Dong J, Chen J, Eastoe J, Li X. Design and optimization of a new self-nanoemulsifying drug delivery system. *J Colloid Interface Sci*. 2009;330(2):443–448.
41. Shakeel F, Ramadan W. Transdermal delivery of anticancer drug caffeine from water-in-oil nanoemulsions. *Colloids Surf B Biointerfaces*. 2010;75(1):356–362.
42. Jang J-H, Jeong S-H, Lee Y-B. Enhanced lymphatic delivery of methotrexate using W/O/W nanoemulsion: in vitro characterization and pharmacokinetic study. *Pharmaceutics*. 2020;12(10):978.
43. Tadros TF. *Emulsion Formation and Stability*. John Wiley & Sons; 2013.
44. Dhaval M, Devani J, Parmar R, Soniwala M, Chavda J. Formulation and optimization of microemulsion based sparfloxacin in-situ gel for ocular delivery: in vitro and ex vivo characterization. *J Drug Deliv Sci Technol*. 2020;55:101373.
45. Romes NB, Wahab RA, Abdul Hamid M, Hashim SE. D-optimal design-assisted Elaeis guineensis leaves extract in olive oil-sunflower seed nanoemulsions: development, characterization, and physical stability. *J Dispers Sci Technol*. 2020;43:1–13.
46. Bhatia G, Zhou Y, Banga AK. Adapalene microemulsion for transfollicular drug delivery. *J Pharm Sci*. 2013;102(8):2622–2631.
47. Warr GG. Shear and elongational rheology of ternary microemulsions. *Colloids Surf a Physicochem Eng Asp*. 1995;103(3):273–279.
48. Villar AMS, Naveros BC, Campmany ACC, Trenchs MA, Rocabert CB, Bellowa LH. Design and optimization of self-nanoemulsifying drug delivery systems (SNEDDS) for enhanced dissolution of gemfibrozil. *Int J Pharm*. 2012;431(1–2):161–175.
49. Parmar N, Singla N, Amin S, Kohli K. Study of cosurfactant effect on nanoemulsifying area and development of lercanidipine loaded (SNEDDS) self nanoemulsifying drug delivery system. *Colloids Surf B Biointerfaces*. 2011;86(2):327–338.
50. Shah N, Seth A, Balaraman R, Sailor G, Javia A, Gohil D. Oral bioavailability enhancement of raloxifene by developing microemulsion using D-optimal mixture design: optimization and in-vivo pharmacokinetic study. *Drug Dev Ind Pharm*. 2018;44(4):687–696.
51. Gonzalez AC, Costa TF, Andrade ZA, Medrado AR. Wound healing-A literature review. *An Bras Dermatol*. 2016;91:614–620.
52. Addis R, Cruciani S, Santaniello S, et al. Fibroblast proliferation and migration in wound healing by phytochemicals: evidence for a novel synergic outcome. *Int J Med Sci*. 2020;17(8):1030.
53. Bahramsoltani R, Farzaei MH, Rahimi R. Medicinal plants and their natural components as future drugs for the treatment of burn wounds: an integrative review. *Arch Dermatol Res*. 2014;306(7):601–617.
54. Vicens-Zygmunt V, Estany S, Colom A, et al. Fibroblast viability and phenotypic changes within glycated stiffened three-dimensional collagen matrices. *Respir Res*. 2015;16(1):1–15.
55. Nakagawa S, Pawelek P, Grinnell F. Long-term culture of fibroblasts in contracted collagen gels: effects on cell growth and biosynthetic activity. *J Investig Dermatol*. 1989;93(6):792–798.
56. Zhang G-Y, Gao W-Y, Li X, et al. Effect of camptothecin on collagen synthesis in fibroblasts from patients with keloid. *Ann Plast Surg*. 2009;63(1):94–99.
57. Padayatty SJ, Katz A, Wang Y, et al. Vitamin C as an antioxidant: evaluation of its role in disease prevention. *J Am Coll Nutr*. 2003;22(1):18–35.
58. Farris PK. Topical vitamin C: a useful agent for treating photoaging and other dermatologic conditions. *Dermatol Surg*. 2005;31:814–818.
59. Jeong J-H, Kim M-B, Kim C, Hwang J-K. Inhibitory effect of vitamin C on intrinsic aging in human dermal fibroblasts and hairless mice. *Food Sci Biotechnol*. 2018;27(2):555–564.
60. Hata RI, Senoo H. L-ascorbic acid 2-phosphate stimulates collagen accumulation, cell proliferation, and formation of a three-dimensional tissue like substance by skin fibroblasts. *J Cell Physiol*. 1989;138(1):8–16.
61. Mohammed BM, Fisher BJ, Kraskauskas D, et al. Vitamin C promotes wound healing through novel pleiotropic mechanisms. *Int Wound J*. 2016;13(4):572–584.
62. Chaitrakoonthong T, Ampornaramveth R, Kamolratanakul P. Rinsing with L-ascorbic acid exhibits concentration-dependent effects on human gingival fibroblast in vitro wound healing behavior. *Int J Dent*. 2020;2020:4706418.
63. Shibuya S, Ozawa Y, Toda T, et al. Collagen peptide and vitamin C additively attenuate age-related skin atrophy in Sod1-deficient mice. *Biosci Biotechnol Biochem*. 2014;78(7):1212–1220.
64. Conti M, Couturier M, Lemonnier F, Lemonnier A. Antioxidant properties of vitamin E and membrane permeability in human fibroblast cultures. In: *Antioxidants in Therapy and Preventive Medicine*. Springer; 1990:125–128.
65. Kiselmann C, Dobler D, Schmidts T, et al. Development of a skin-friendly microemulsion for dermal allergen-specific immunotherapy. *Int J Pharm*. 2018;550(1–2):463–469.
66. Tanaka M, Koyama Y-I, Nomura Y. Effects of collagen peptide ingestion on UV-B-induced skin damage. *Biosci Biotechnol Biochem*. 2009;73(4):930–932.
67. Roewert-Huber J, Stockfleth E, Kerl H. Pathology and pathobiology of actinic (solar) keratosis–an update. *Br J Dermatol*. 2007;157:18–20.
68. Fernandes TR, Santos I, Korinsfky JP, Silva BSL, Carvalho LO, Plapler H. Cutaneous changes in rats induced by chronic skin exposure to ultraviolet radiation and organophosphate pesticide1. *Acta Cirúrgica Brasileira*. 2014;29:07–15.

69. Maia Campos PM, Melo MO, Siqueira Cesar FC. Topical application and oral supplementation of peptides in the improvement of skin viscoelasticity and density. *J Cosmet Dermatol*. 2019;18(6):1693–1699.
70. Lin J-Y, Selim MA, Shea CR, et al. UV photoprotection by combination topical antioxidants vitamin C and vitamin E. *J Am Acad Dermatol*. 2003;48(6):866–874.
71. Darr D, Dunstonz S, Faust H, Pinnell S. Effectiveness of antioxidants (vitamin C and E) with and without sunscreens as topical photoprotectants. *Acta Derm Venereol*. 1996;76:264–268.